

High Power Interferometric Phase Measurement Limited by Quantum Noise and Application to Detection of Gravitational Waves

P. Fritschel, G. González,* B. Lantz, P. Saha,[†] and M. Zucker

Department of Physics and Center for Space Research, Massachusetts Institute of Technology, Cambridge, Massachusetts 02139

(Received 17 November 1997)

Interferometric detection of gravitational waves at levels of astrophysical interest is expected to require measurement of optical phase differences of $\leq 10^{-10}$ rad. To achieve this sensitivity the measurement must be made at the quantum (shot noise) limit. We have built a laboratory-scale interferometer to investigate limits to sensing the phase at this level, and obtained, with 70 W of circulating power, a phase sensitivity limited by shot noise of 3×10^{-10} rad/ $\sqrt{\text{Hz}}$ at frequencies above 1.5 kHz. We describe the experiment and discuss the implications for the Laser Interferometer Gravitational-Wave Observatory (LIGO). [S0031-9007(98)05769-X]

PACS numbers: 04.80.Nn, 07.60.Ly, 42.50.Ar, 95.55.Ym

Interferometric gravitational wave detectors now in construction [1,2] employ variants of a Michelson interferometer to detect astrophysical gravitational wave strains. A gravitational wave, described by its dimensionless strain amplitude h and Fourier frequency f , produces a relative phase shift ϕ_d between the optical fields traversing the two orthogonal arms of the interferometer. This shift is detected as an intensity change in the interference between the fields. The detectors are designed to be quantum noise limited in a wide frequency range—as determined by the Poisson statistics of photon detection (“shot” noise). For light in a coherent state, the amplitude spectral density of phase fluctuations that would produce a signal power equal to that produced by the shot noise is $\dot{\phi}_d(f) = \sqrt{4\pi\hbar\nu_l/\eta P}$, where ν_l is the optical frequency, P is the power incident on the beam splitter, η is the quantum efficiency of the photodetector, and \hbar is Planck’s constant. This “phase noise,” in turn, limits the strain sensitivity as $\tilde{h}(f) = \dot{\phi}_d(f)(\delta\phi_d/h)^{-1}$, where $(\delta\phi_d/h)$ is the transfer function of the interferometer (which is generally frequency dependent). Where resonant Fabry-Perot cavities are used in the arms [as in the Laser Interferometer Gravitational-Wave Observatory (LIGO)], this is given by $|(\delta\phi_d/h)| \approx (8\pi\nu_l\tau_s)/\sqrt{1+(4\pi f\tau_s)^2}$, where f is the gravitational wave frequency, and τ_s is the storage time of the Fabry-Perot cavities. In LIGO $\tau_s = 0.88$ msec, $\nu_l = 2.8 \times 10^{14}$ Hz, and the transfer function is $|(\delta\phi_d/h)| \approx 6.2 \times 10^{12}$ rad at $f = 0$. LIGO interferometers are designed to be shot noise limited for frequencies $f > 150$ Hz, where a strain sensitivity of $\tilde{h}(150 \text{ Hz}) \approx 3 \times 10^{-23}$ Hz $^{-1/2}$ will allow detection of gravitational waves at a level $h_{\text{rms}} \approx 10^{-21}$ —a sensitivity of astrophysical interest [3]. The implied phase sensitivity of $\dot{\phi}_d(f > 150 \text{ Hz}) = 7 \times 10^{-11}$ rad/ $\sqrt{\text{Hz}}$ requires at least 100 W of power at the beam splitter; when feasible quantum efficiency and other details of the full sensing system are taken into account, a power level closer to 300 W is needed to achieve the strain sensitivity goal. Such high power in a stable, single frequency laser

beam can currently be obtained only using a “power recycling” technique [4]. This technique takes advantage of operating the interferometer on a “dark fringe,” where the average arm length difference is controlled so that the intensity at the output is a minimum. At this point, the optical system acts as a mirror and reflects most of the light back toward the laser. By including a partially transmissive mirror between the laser and the beam splitter, an optical cavity is formed that increases the power at the beam splitter. The “recycling gain” G is the ratio of the power incident on the beam splitter to the input power. While power recycling has been demonstrated on tabletop [5] and suspended [6] interferometers, which achieved recycling gains as high as 300, the best phase sensitivity, $\dot{\phi}_d(f > 400 \text{ Hz}) \approx 3 \times 10^{-9}$ rad/ $\sqrt{\text{Hz}}$, was achieved in an unrecycled Michelson interferometer [7]. We present here an experiment employing power recycling on a suspended Michelson interferometer to achieve a recycling gain of 450 and a phase sensitivity limited by photon shot noise of $\dot{\phi}_d(f > 1.5 \text{ kHz}) \approx 3 \times 10^{-10}$ rad/ $\sqrt{\text{Hz}}$.

Figure 1 shows a simplified schematic, and Table I gives significant parameters of the system [8]. The power-recycled Michelson configuration with unbalanced arm lengths was chosen to make the phase sensing similar to that of LIGO. On the other hand, we have reduced the sensitivity to mirror motion by foregoing resonant arm cavities. The light source is a single frequency, 514 nm wavelength argon ion laser [9].

The mirrors and beam splitter are fused silica with multilayer dielectric coatings, and are each suspended by a loop of steel wire. The position of each optic with respect to its suspension support structure is sensed optically. These signals are used to actively damp four rigid-body modes (an axial and a transverse mode at 1 Hz, and two angular modes at 0.45 Hz), using coils mounted on the support structure to produce forces on magnets bonded to the optic.

The arm mirrors and the beam splitter are located on one optical platform, seismically isolated both passively (with a four-layer seismic isolation stack [10]) and actively

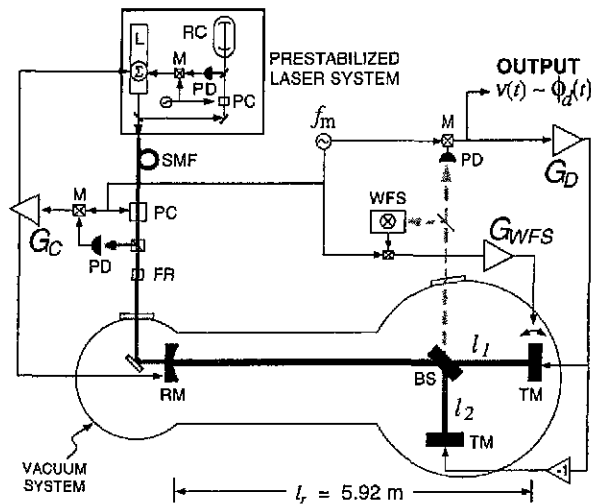


FIG. 1. Simplified schematic of the interferometer. Symbols are as follows: PC: Pockels cell; FR: Faraday isolator; TM: test mass (high reflector); BS: beam splitter; RM: recycling mirror; SMF: single mode fiber; RC: reference cavity; M: mixer; WFS: wave front sensor; L: laser; G_D : differential length controller; G_C : common length and frequency trim controller; and G_{WFS} : alignment controller.

(using commercial low-frequency isolators). The recycling mirror is on a separate optical platform, similarly isolated. The platforms and the 6 m path between them are enclosed in a high-vacuum chamber.

The laser frequency is actively stabilized with respect to a stable reference cavity [11]. The light is transmitted to the interferometer through a single-mode optical fiber used to stabilize the beam direction. An electro-optic phase modulator, driven sinusoidally at f_m with a relatively small amplitude, produces first-order modulation sidebands at $\nu_l \pm f_m$. The modulation frequency is chosen at $f_m = c/2l_r$, where l_r is the average distance from the two arm mirrors to the recycling mirror, such that these sidebands are resonant in the recycling cavity along with the carrier. The light exiting the Michelson antisymmetric port and the light reflected by the interferometer are detected with tuned photodetectors; each photodetector signal is demodulated at f_m to give a zero-crossing error signal. The antisymmetric port error signal is primarily sensitive to the Michelson differential phase, and

TABLE I. Significant parameters of the interferometer.

Parameter	Value
Mirror dimensions (diameter \times thickness)	76.2 mm \times 25.4 mm
Recycling mirror transmission (T_r); radius of curvature	0.82%; 10 m concave
Recycling cavity length, $l_r = (l_1 + l_2)/2$	5.92 m
Modulation frequency, f_m ; depth	25.22 MHz; 0.55 rad
Michelson asymmetry, $\Delta l = (l_1 - l_2)$	20.8 cm
Input power, P_{in}	190 mW
Recycling gain, G	450

the reflected port error signal is primarily sensitive to the common (recycling cavity) phase; they are used in control loops to maintain the dark fringe and cavity resonance conditions, respectively.

The Michelson phase error signal depends on the existence of a macroscopic asymmetry Δl between the arms [12]. Because of this unbalance, when the carrier light is at the dark fringe, the modulation sidebands do not completely destructively interfere, and sideband power is transmitted to the antisymmetric output; the size of the asymmetry is chosen so that most of the incident sideband power is transmitted to the output. The sideband field interferes with the carrier field produced by small deviations from the dark fringe, creating an amplitude-modulated photocurrent proportional to the phase deviation. The demodulated signal is used in a feedback loop to maintain the carrier at the dark fringe; correction signals are sent differentially to the actuators on both Michelson mirrors. The loop has a bandwidth of ~ 300 Hz, and reduces differential length fluctuations from ~ 35 nm rms (uncontrolled) to ~ 3 pm in operation.

For small deviations from resonance, the signal detected in reflection is proportional to the "common mode" round-trip phase $\phi_c = 4\pi\nu l_r/c$. This works similarly to standard cavity reflection locking [13], with the difference that here the carrier and sidebands are simultaneously resonant. The Michelson asymmetry ensures that the round-trip loss for the sidebands is higher than that for the carrier, so deviation from resonance produces a large phase shift on the carrier than on the sidebands. This phase dispersion results in an amplitude modulation on the light that is proportional to the deviation. The common mode servo serves two functions: to maintain resonance of the cavity, and to suppress frequency fluctuations. Fluctuations in the common mode phase are dominated at low frequencies by variation of the length l_r , and at a high frequencies by fluctuations in the laser frequency. The demodulated common mode signal is, therefore, used to correct the recycling cavity length at low frequencies (via the recycling mirror actuators), and to correct the laser frequency at high frequencies (by adding a correction signal to the laser prestabilization control [14]). At frequencies above the "crossover," where these paths have equal effect (~ 100 Hz), this further stabilizes the laser frequency (the length of the suspended cavity is more stable than the reference cavity at these frequencies). The bandwidth of the common mode control loop is about 20 kHz.

The alignment of the Michelson interferometer is also sensed interferometrically and controlled. A quadrant photodetector detects spatial asymmetries in the rf amplitude modulation of a small fraction of the antisymmetric output beam which are produced by wave front misalignment [15,16]. A feedback control signal corrects the angular orientation of one of the Michelson mirrors. Active alignment control is indispensable, since fluctuations in these angles result in power loss and a corresponding reduction in the recycling gain. Typical uncontrolled

alignment fluctuations of tens of μ radians reduce the average recycling gain to $\sim \frac{1}{3}$ its maximum value; with the alignment control active, variations in the recycling gain from misalignment remain less than $\sim 1\%$.

Figure 2 shows the spectrum of apparent fluctuations in the Michelson phase difference ϕ_d , expressed as the equivalent difference between the round-trip phase shifts in the two arms. This spectrum is derived from the demodulated antisymmetric output signal by subtracting, in quadrature, the photodetection electronics noise, which is independently measured at approximately 10 dB below the operating level, and then applying a correction for the measured open-loop gain (the loop suppresses the signal at frequencies below the unity gain frequency of ~ 300 Hz). The spectrum is calibrated by adding a known sinusoidal force at 2 kHz to one of the Michelson mirrors, via its electromagnetic actuators.

The phase noise spectrum has three distinct regions. Above 1.5 kHz, the mean value of the nearly "white" spectral density is $\tilde{\phi}_d(f) = (2.7 \pm 0.3) \times 10^{-10}$ rad/ $\sqrt{\text{Hz}}$. This region is dominated by shot noise, as we will discuss below. Resonant peaks between 1 kHz and 1.5 kHz are due to mechanical flexure modes of the actuator magnet assemblies bonded to the mirrors. Their frequencies, widths, and amplitudes are consistent with mirror recoil from the expected Brownian motion of these assemblies. The 2 kHz peak is a 1.9×10^{-7} rad rms calibration signal applied as a force to one mirror through its electromagnetic actuator.

Between 100 Hz and 1 kHz the phase difference is statistically correlated with the common mode loop error signal (the cross-spectral coherence function ranges from unity at 100 Hz to 0.5 at 500 Hz). The phase noise in

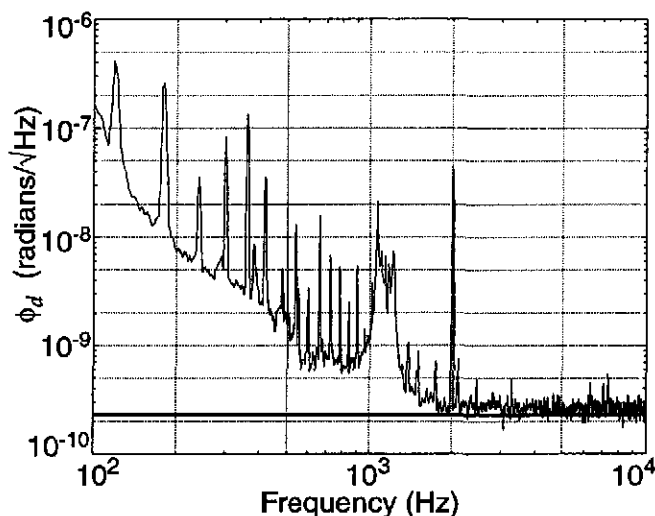


FIG. 2. Amplitude spectral density of the equivalent Michelson phase difference ϕ_d . The predicted shot noise limited level for the measured system parameters is indicated by the straight solid line. The peak at 2 kHz is a calibration line. The plot is a composite of two fast Fourier transforms; the resolution bandwidth in the 1.2–10 kHz band is 18.7 Hz, and in the 100 Hz–1.2 kHz band is 4.7 Hz.

the 100 Hz–1 kHz region was also shown to decrease proportionally with increasing loop gain in the common mode control. This behavior leads us to conclude that the measured phase noise in this region is dominated by the effect of residual laser frequency noise. Because of the asymmetry Δl , we, in fact, expect a significant first-order sensitivity of the phase ϕ_d to changes in laser frequency: $\phi_d = 4\pi\Delta l\delta\nu_l/c = 8.7 \times 10^{-9}\delta\nu_l$ rad/Hz. The common mode control configuration used here imposed a limitation to further suppression of frequency noise in this band. The laser control path has a relatively small dynamic range ($\pm \sim 30$ kHz) for making frequency corrections, and so the large low-frequency cavity length correction signals (equivalent to $\pm \sim 100$ MHz of frequency change) must be strongly high-pass filtered in the laser path. This prevents the crossover frequency from being lower than ~ 100 Hz. Above the crossover, it is only the ratio of the gain in the laser path to that in the cavity length path that is effective in suppressing the input frequency noise; this ratio does not become very large until well above the crossover frequency.

The recycling gain is an important factor determining the sensitivity, but the power in the cavity is not directly measurable. Instead, the recycling gain is inferred from a "cavity ringdown" loss measurement. By square-wave modulating the input power with a $\sim 10\%$ depth, and measuring the exponential time constant of the light transmitted through one of the arm mirrors, we infer a round-trip loss for the carrier of $L_0 = 9 \times 10^{-3}$ (corresponding to 800 ppm in addition to the known recycling mirror transmission). The loss is related to the cavity finesse for the carrier F_c by $F_c = 2\pi/L_0$. In the limit where the input beam is perfectly matched to the cavity mode, this gives a recycling gain $G = 2F_c/\pi = 450 \pm 50$. Measurement of the power transmitted by one of the arm mirrors when the system is on and off resonance gives a consistent recycling gain figure.

It is interesting to compare our sensitivity with the shot noise limited phase noise in an ideal system—one with no losses (other than the recycling mirror transmission), and quantum efficiency and mode coupling of 100%. The shot noise limit to the phase in this case is calculated as

$$\tilde{\phi}_d(f) = \sqrt{\frac{3h\nu_l}{P_{bs}}} \quad (1)$$

This differs from the expression given in the first paragraph by a factor of $\sqrt{3/2}$, due to the fact that the power at the photodetector is not stationary, but rather varies at $2f_m$, since it is due entirely to the modulation sidebands [17]. In this limit the power at the beam splitter P_{bs} is determined only by the recycling mirror transmission: $P_{bs} = 4P_{in}/T_r$. For our input power and recycling mirror, the ideal phase sensitivity would thus be $\tilde{\phi}_d(f) = 1.1 \times 10^{-10}$ rad/ $\sqrt{\text{Hz}}$.

Losses and other imperfections both decrease the signal sensitivity—by reducing the effective power at the beam splitter, and increase the noise—by increasing the average

power at the antisymmetric output. Imperfect interference of the carrier at the beam splitter, for example, causes both signal loss and extra shot noise-generating power at the output. The quality of the interference is described by the contrast $C \equiv (P_{bs} - P_{as})/(P_{bs} + P_{as})$, where P_{bs} is the carrier power incident on the beam splitter and P_{as} the carrier power at the antisymmetric output. The contrast determines the optimal rf modulation index to maximize the signal-to-(shot)noise ratio. So optimized, the shot noise limited sensitivity in the presence of losses is found to be [8]

$$\tilde{\phi}_d(f) = F_{ns} \sqrt{\frac{2h\nu_l}{\eta P_{bs}} \left(1 + \frac{1-C}{4 \sin^2(2k_m \Delta l)} R_{bs} \right)}, \quad (2)$$

where F_{ns} is the nonstationary correction factor, $k_m (= 2\pi f_m/c)$ is the modulation wave number, and R_{bs} is the ratio of power in the carrier to that in the sidebands at the beam splitter. Since we cannot measure the carrier power at the beam splitter directly, we express it in terms of accessible parameters. Using an optical spectrum analyzer, we measure the ratio of the power in the carrier to that in the sidebands at various points; making this measurement on the light transmitted by one of the arm mirrors gives $R_{bs} = 35 \pm 4$. The effective beam splitter power, expressed in terms of a photocurrent, is $\eta P_{bs}/h\nu_l = \bar{i}_{as}(R_{bs}/R_{as} - 1) \sin^{-2}(2k_m \Delta l)$, where $\bar{i}_{as} = 4.2$ mA is the average photocurrent, and $R_{as} = 0.16 \pm 0.02$ is the carrier-to-sideband power ratio at the antisymmetric output (also measured with an optical spectrum analyzer). The nonstationary factor F_{ns} and the contrast C can also be expressed in terms of these ratios, $F_{ns} = \sqrt{(3/2 + R_{as})/(1 + R_{as})}$ and $1 - C = 2R_{as} \sin^2(2k_m \Delta l)/R_{bs}$. Our measurements give $F_{ns} = 1.20 \pm 0.02$, $1 - C = 1.0 \times 10^{-4}$, and a predicted phase sensitivity of $\tilde{\phi}_d(f) = (2.3 \pm 0.3) \times 10^{-10}$ rad/ $\sqrt{\text{Hz}}$ about twice the ideal limit given by Eq. (1). The factor in Eq. (2), due to imperfect contrast, is only 1.07; most of the remaining difference between the ideal and predicted sensitivity results from reduced effective beam splitter power, due to a quantum efficiency of $\sim 50\%$, a mode mismatch of 10%, and other optical losses.

We independently verify that the high frequency noise is dominated by shot noise by separately illuminating the photodetector with a blackbody thermal spectrum, producing the same average photocurrent (4.2 mA) as in operation. We then measure the voltage spectral density at the readout point, subtract electronics noise in quadrature, and multiply the result by the nonstationarity factor F_{ns} . The resulting (white) spectrum is within 20% of the level measured in Fig. 2.

The phase noise spectrum presented here is well characterized for frequencies between 100 Hz and 10 kHz, and is shot noise limited at the level of $\tilde{\phi}_d(f) = (2.7 \pm 0.3) \times 10^{-10}$ rad/ $\sqrt{\text{Hz}}$ above 1.5 kHz. We have demonstrated a phase sensitivity close to that required in initial LIGO interferometers, and have an understanding of the sources of error in the measurements which lends confidence to achieving the initial LIGO sensitivity. We are currently engaged in repeating the measurements using a 1.06 μm Nd:YAG laser source, the wavelength, and laser type that will be used in LIGO.

We thank the entire LIGO team at Caltech and MIT for assistance and support. We especially thank D. Shoemaker, S. Whitcomb, and R. Weiss for useful technical advice. We are very grateful for assistance with the active alignment system to N. Mavalvala and D. Sigg. This work was supported by NSF Grant No. PH-9210038.

*Current address: Pennsylvania State University, Department of Physics, 104 Davey Laboratory, University Park, PA 16802.

†Current address: Imatron Inc., 389 Oyster Pt. Blvd., S. San Francisco, CA 94080-1998.

- [1] A. Abramovici *et al.*, *Science* **256**, 325 (1992).
- [2] A. Giazotto, in *Proceedings of the First Edoardo Amaldi Conference on Gravitational Wave Experiments, Frascati, 1994*, edited by E. Coccia, G. Pizzella, and F. Ronga (World Scientific, Singapore, 1995); K. Danzmann, *ibid.*
- [3] K. Thorne, in *300 Years of Gravitation*, edited by Hawking and W. Israel (Cambridge University Press, Cambridge, 1987).
- [4] R. Drever *et al.*, in *Quantum Optics, Experimental Gravity and Measurement Theory* (Plenum, New York, 1983); H. Billing *et al.*, *ibid.*
- [5] C. N. Man *et al.*, *Phys. Lett. A* **148**, 8 (1990).
- [6] D. Schnier *et al.* (to be published).
- [7] D. Shoemaker *et al.*, *Phys. Rev. D* **38**, 423 (1988).
- [8] P. Saha, Ph.D. thesis, Massachusetts Institute of Technology, 1997.
- [9] After this experiment started, LIGO switched to Nd:YAG lasers at 1.06 μm .
- [10] J. Giaime, P. Saha, and D. Shoemaker, *Rev. Sci. Instrum.* **67**, 208 (1996).
- [11] G. A. Kerr *et al.*, *Appl. Phys. B* **37**, 11 (1985).
- [12] L. Schnupp, Max Planck Institute for Quantum Optics, Garching, Germany (private communication).
- [13] R. Drever *et al.*, *Appl. Phys. B* **31**, 97 (1983).
- [14] S. Kawamura, A. Abramovici, and M. Zucker, *Rev. Sci. Instrum.* **68**, 223 (1997).
- [15] E. Morrison *et al.*, *Appl. Opt.* **33**, 5041-5049 (1994).
- [16] Y. Hefetz, N. Mavalvala, and D. Sigg, *J. Opt. Soc. Am. B* **14**, 1597-1605 (1997).
- [17] T. M. Niebauer *et al.*, *Phys. Rev. A* **43**, 5022 (1991).